Coil−Stretch Transition of High Molar Mass Polymers in Packed-Column Hydrodynamic Chromatography

Yonggang Liu,* Wolfgang Radke, and Harald Pasch*

Deutsches Kunststoff-Institut (German Institute for Polymers), Schlossgartenstr. 6, D-64289 Darmstadt, Germany

Received May 9, 2005; Revised Manuscript Received June 30, 2005

ABSTRACT: The elution behavior of high molar mass polystyrene (PS) in packed-column hydrodynamic chromatography (HDC) was studied at different eluent flow rates by using a multiangle laser light scattering (MALLS) detector. A chromatography mode transition from HDC to slalom chromatography (SC) was observed for high molar mass PS samples with abnormal elution behaviors. The critical polymer size $R_{g,c}$ of the HDC to SC transition was determined by the plateau value of the R_g-V_e curve for the earliest eluting polymer fraction. The dependence of $R_{g,c}$ on flow rate was explained by coil−stretch transitions of the polymer molecules in elongational flow through the packed column. The transition of chromatography mode may provide a new method to study the coil−stretch transition of polymers in elongational flow through packed beds. For high molar mass polymer samples, HDC must be performed at flow rates sufficiently low that the elongational rate in the column is less than the critical strain rate for coil−stretch transitions to occur for all species in the sample.

Introduction

Size-separation techniques, such as size exclusion chromatography (SEC),[1] field-flow fractionation (FFF),[2] and the less known hydrodynamic chromatography (HDC),[3] are convenient and quick methods to determine the size and size distribution of macromolecules. HDC is a technique originally developed for the size determination of polymer latices[4] and was later applied for the analysis of high molar mass macromolecules.[5−8] The separation in HDC is due to the exclusion of solute molecules from the low-velocity regions near the capillary wall or particle surface in a Poiseuille flow profile. A larger macromolecule will be more excluded from the low-velocity regions near the wall than a smaller macromolecule. Hence, the larger macromolecule experiences a higher mean eluent velocity and elutes earlier than the smaller macromolecule; i.e., the elution order of macromolecules in HDC is the same as in SEC, which had been observed in both packed-column and microcapillary HDC.[5−11] It was found that in HDC columns packed with 1−3 μm nonporous particles the relative peak retention time of lower molar mass polymers ($<\sim$1 M) showed no flow rate dependence, while the relative peak retention time of higher molar mass polymers ($>\sim$1 M) increased with increasing flow rate, and this effect was more prominent for larger polymers.[7−10] It was also found that high molar mass polymers ($>\sim$1 M) of different molar masses coeluted from HDC columns packed with 1 μm nonporous particles.[10] The abnormal elution behavior of high molar mass polymers was explained by shear deformation and degradation at high flow rates. However, the appearance of double peaks at high flow rate for high molar mass polystyrene (PS) was not assigned to a specific effect by the authors.[9]

For a polymer molecule in elongational flow, a coil−stretch transition occurs when the Deborah number (D_e), which is the product of the longest relaxation time of the polymer, τ, and the strain rate of the flow, $\dot{\epsilon}$, is larger than a threshold value B.[12] B was predicted to be 0.5 by theory[13] and was verified by different experiments based on light scattering,[14] birefringence,[15] and viscoelastic flow[16] and more recently by direct observation of fluorescently labeled DNA.[17−20] The onset of polymer stretching occurs at a critical strain rate $\dot{\epsilon}_c$ of

$$\dot{\epsilon}_c = \frac{B}{\tau} \tag{1}$$

For $\dot{\epsilon} < \dot{\epsilon}_c$, the polymer is in a "coiled" state. As $\dot{\epsilon}$ increases above $\dot{\epsilon}_c$, the hydrodynamic force exerted across the polymer just exceeds the linear portion of the polymer's entropic elasticity, and the polymer stretches until its nonlinear elasticity limits the further extension of this "stretched" state. A strong heterogeneity in the dynamics and conformations of individual chains in elongational flow was observed, while the steady-state extension of the polymer increased rapidly at $D_e > 0.4$ to a asymptotic value very close to the full contour length of the chain at large D_e.[17−20]

In an early work to separate large DNA fragments using SEC columns, a new chromatography mode, slalom chromatography (SC), was observed.[21] It was found that for large DNA fragments of 10−40 kbp (1 kbp = 1000 base pairs, one base pair has a mass of $\sim$660[22]) the smaller fragments were eluted faster than the larger fragments, while normal SEC separation was observed for DNA fragments smaller than 5 kbp. It was explained that DNA strands were stretched because of the relatively high flow rate. They were too large to permeate the pores and could only pass through the narrow channels between closely packed spherical particles. Since the channels were extremely tortuous, the molecules must turn very frequently and thus were retarded. The longer the macromolecule chain, the more difficult it was to pass through the channels; i.e., the elution order in SC was opposite to SEC and HDC. This SEC → SC transition was found to be dependent on the packing particle size, the flow rate, molecular size, temperature, and solvent viscosity.[23,24] The HDC → SC

* Corresponding author: e-mail ygliu2000@yahoo.com (Liu), hpasch@dki.tu-darmstadt.de (Pasch).

10.1021/ma050964g CCC: $30.25
Published on Web 07/30/2005

Table 1. Molar Masses of PS Standards as Given by Suppliers

sample	supplier	$M_{w,LS}$ (kg/mol)	M_w[f] (kg/mol)	M_w/M_n[f]
PS125K	PSS[a]		125	1.04
PS200K	PC[b]		200	<1.06
PS226K	PSS[a]		226	1.06
PS564K	PSS[a]		564	1.03
PS1M	PSS[a]		1070	1.06
PS2M	PSS[a]		2530	1.04
PS4M	PSS[a]		4060	1.15
PS5M	PL[c]	4930[d]	4843	1.06
PS7M	PL[c]		7700	
PS8M	PSS[a]		8090	1.17
PS10M	PL[c]	8280[e]	9225	1.06
PS16M	PSS[a]		16800	1.33
PS14M	PL[c]	19825[d]	14370	1.06

[a] Polymer Standards Service GmbH. [b] Pressure Chemical Co. [c] Polymer Laboratories Ltd. [d] $M_{w,LS}$ determined by static light scattering at several low angles and concentrations. [e] $M_{w,LS}$ determined by SEC coupled with light scattering at 15°. [f] M_w and M_w/M_n determined by SEC.

transition was also observed for large DNA recently; the migration dependence on the flow rate for different species showed a transition from HDC at low flow rate to SC at high flow rate.[25]

For high molar mass polymers flowing through HDC columns at a high flow rate with an abnormal elution behavior, the calculated average D_e was found to be larger than 0.5,[5,26] indicating the existence of a coil−stretch transition. However, for synthetic polymers which are not monodisperse like DNA, such a SEC → SC or HDC → SC transition induced by coil−stretch transition was concealed by the different behaviors (coiled, stretched, degraded) of the components with different sizes and was not observed previously or at least was not explained clearly.

In the present paper, a series of PS with different molar masses were studied by packed-column HDC coupled with a multiangle laser light scattering (MALLS) detector at different flow rates. The flow rate dependence of the HDC → SC transition for high molar mass PS was observed and explained by the coil−stretch transition of the polymer molecules in elongational flow through the packed column. This transition of chromatography mode may provide a new method to study the coil−stretch transition of polymers in elongational flow through packed beds.

Experimental Part

Technical grade tetrahydrofuran (THF) from BASF (Ludwigshafen, Germany) was distilled before use.

PS standards with M_w ranging from 125K to 16.8M were obtained from Polymer Standards Service GmbH (Mainz, Germany), Pressure Chemical Co. (Pittsburgh, PA), and Polymer Laboratories Ltd. (Shropshire, UK). The molar mass data given by the supplier are listed in Table 1.

An ISCO 100DX syringe pump (Lincoln, NE) providing constant flow rates between 0.01 μL/min and 50 mL/min was employed. The eluent flow rates used ranged from 0.025 to 1.00 mL/min. The concentration detector, a Waters 486 UV detector (Milford, MA), was placed before a Wyatt DAWN EOS MALLS detector (Santa Barbara, CA) with a 690 nm laser source and 17 scattering angles at 16.8, 23.2, 31.3, 38.8, 45.8, 53.8, 61.6, 70.4, 80.2, 90.0, 99.8, 109.6, 119.5, 129.6, 138.9, 147.4, and 155.4°. Two columns (300 × 4.6 mm) packed with 15 μm cross-linked polystyrene−divinylbenzene nonporous particles (PL Ltd.) were placed in an oven kept at 35 °C.

Sample solutions were prepared at concentrations of 0.05−0.2 g/L in THF, depending on molar mass. The injection volume was 3.2 μL. The injected polymer mass was kept at such a low level to avoid overloading the column.

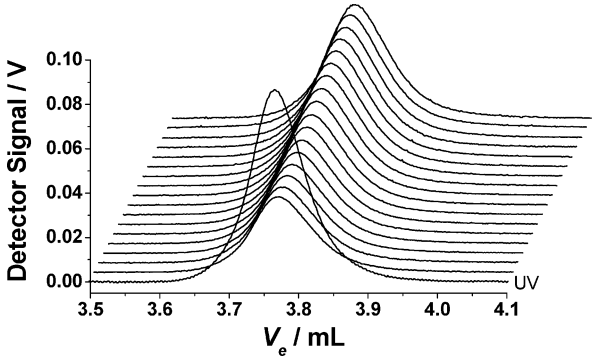

Figure 1. HDC-MALLS chromatogram of PS1M obtained by columns packed with 15 μm particles at a flow rate of 0.10 mL/min. The lines are signals from the LS detector of 17 angles (from top to bottom is in the order of increasing angle) and the UV detector.

Wyatt Astra software was used for data acquisition and analysis. Of the four fit methods provided by the Astra software, namely Debye, Zimm, Berry, and Random coil fit method, the Random coil method was used in this study, since it gave the most accurate results for high molar mass polymers.[27]

Results and Discussion

Figure 1 shows the UV and LS traces at different angles obtained at flow rate of 0.10 mL/min for PS1M at an injected concentration of 0.14 g/L. The light scattering intensity decreases with increasing scattering angle. The calculated molar mass M and radius of gyration R_g as functions of elution volume V_e, as well as polymer concentration at each V_e, are shown in Figure 2. It can be seen that the LS detector signal is slightly broader than that of the UV detector. This is due to band broadening in the MALLS flow cell as a consequence of its large volume of 70 μL. Consequently, the calculation of M at each elution slice from the concentration (UV) signal and the broadened light scattering signal will overestimate the molar mass of the fractions at both ends and underestimate the molar mass of the fractions at the central portion of the chromatogram. Hence a V-shaped $M-V_e$ curve was obtained, as shown in Figure 2a. However, calculation of R_g at each elution slice only requires the angular dependence of the light scattering intensity of the eluted fraction. It is independent of the polymer concentration used. Thus, the correct R_g-V_e curve can still be obtained despite the band broadening in the MALLS flow cell, as shown in Figure 2b.

Figure 3 shows the chromatogram of PS10M at an injected concentration of 0.07 g/L obtained at flow rate of 0.10 mL/min. A much larger angular dependence of the light scattering signals is observed compared with that of PS1M, owing to its larger size. It should be noted that the LS signal decreased rapidly with increasing scattering angle in the low angle region, while it decreases only slightly in the high angle region. As shown in Figure 3, the scattering intensity at 90° is only ~20% of that at 16.8°. For such a high molar mass polymer, it is the data at the low angle region that determine the accuracy of the obtained results. The data at the high angle give no significant contribution to the quality of the results, although the Random coil fit method was used. It should be noted that the Random

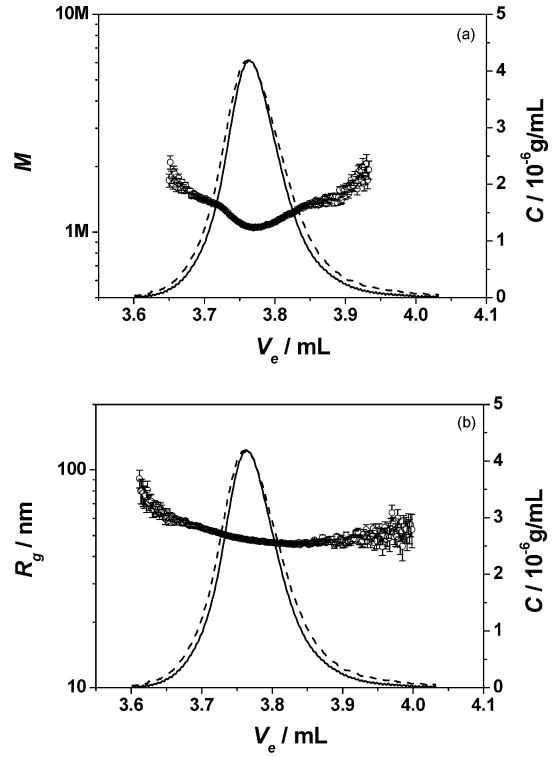

Figure 2. M (a) and R_g (b) as functions of V_e for PS1M obtained by columns packed with 15 μm particles at a flow rate of 0.10 mL/min. The solid lines are polymer concentration at each V_e as calculated from the UV detector signal, while the dashed lines are the LS signal at scattering angle of 90° at each V_e normalized to the same peak height as concentration.

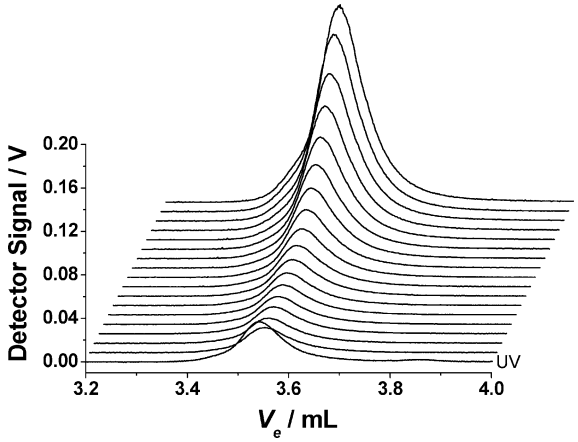

Figure 3. HDC-MALLS chromatogram of PS10M obtained by columns packed with 15 μm particles at a flow rate of 0.10 mL/min. The lines are signals from the LS detector of 17 angles (from top to bottom is in the order of increasing angle) and the UV detector.

coil fit method uses the particle scattering function $P(\theta)$ of a random coil in a Θ solvent to fit the experimental data.

$$P(\theta) = \frac{2}{u^2}(e^{-u} - 1 + u) \qquad (2)$$

where $u = q^2R_g^2$, $q = 4\pi/\lambda \sin(\theta/2)$, λ is the wavelength of the incident light in the solution, and θ is the scattering angle. However, it underestimates the actual particle scattering function of a random coil in a good solvent at large u values ($u > 10$) for large coils at high angles.[28,29] As a result, it will underestimate the molar mass and radius of gyration of a large polymer if these deviating high angle data are included in curve fitting, which was verified by selecting the used angles artificially. In this study, for PS samples having a molar mass of less than 5.3M, all angles were used for fitting by the Random coil fit method; for PS samples having a molar mass higher than 8M, only the light scattering data at angles up to 90° (10 angles) were used; for PS7M, the lowest 11 angles were used.

Tables 2 and 3 summarize the weight-average molar masses, M_w, and z-average radii of gyration, $R_{g,z}$, of PS samples as determined by HDC-MALLS at different flow rates. Figure 4 shows M_w and $R_{g,z}$ as functions of flow rate Q for all PS samples. For smaller polymers (<2.77M), M_w obtained at different flow rates were identical. For all PS with M_w < 2.77M, the average value of M_w was taken over all flow rates, as listed in the last column of Table 2. For larger polymers (>4.92M), M_w obtained at high flow rate (>0.10 mL/min) showed a tendency of decreasing with increasing flow rate. This might be partially due to the errors coming from that relative few data points acquired and the baseline noise of UV detector at high flow rates, but it is probably due to shear deformation and/or degradation, especially for PS with molar masses larger than 10M. For all PS with M_w > 4.92M, the average value of M_w was taken over flow rates less than or equal to 0.10 mL/min, as also listed in the last column of Table 2. $R_{g,z}$ had the same trend as M_w and was treated in the same way. The results are listed in the last column of Table 3. Figure 5a shows the log $R_{g,z}$−log M_w relationship for all PS samples using the average M_w and $R_{g,z}$. A relationship of R_g (nm) = $0.139M^{0.588}$ was obtained, which agreed well with the reference data,[30−32] indicating that correct M_w and $R_{g,z}$ of the whole samples can be obtained, despite additional slight band broadening in MALLS flow cell. Figure 5b shows the log $R_{g,z}$−log M_w relationship for all PS samples obtained at different flow rates. The data obtained at different flow rates also result in a common line.

The dependence of M_w and $R_{g,z}$ on flow rate proved changes of high molar mass PS in flowing through the packed column. The analysis of the M−V_e or R_g−V_e relationships of PS samples at different flow rates may provide direct proof on shear deformation or degradation in HDC columns. However, the correct M−V_e curve cannot be obtained due to the band broadening in the MALLS flow cell, as we had discussed above. The R_g−V_e curve, which is independent of the band broadening in the MALLS flow cell, was used to study the flow rate effect.

R_g as a function of V_e for PS1M obtained at flow rates of 0.025, 0.05, 0.10, 0.30, 0.50, and 1.00 mL/min are shown in Figure 6. This sample eluted from the HDC column at nearly identical elution volumes, showing no flow rate dependence. The obtained R_g−V_e relationships at different flow rates also superimpose well. This agrees with the independence of the obtained M_w and $R_{g,z}$ on flow rate (Tables 2 and 3). A similar independence of elution behavior on flow rate was observed for PS up to M_w = 5.21M. In contrast, for PS7M, -8M, and -10M, a slight flow rate dependence of the chromatogram and the R_g−V_e curve is found. As shown in Figure 7, the chromatograms of PS10M moved to higher elution volumes with increasing flow rates. It is very interesting

Table 2. M_w of PS Standards Determined by HDC-MALLS at Different Flow Rates

	M_w (kg/mol) at flow rate (mL/min) of						
sample	0.025	0.05	0.10	0.30	0.50	1.00	av M_w[a] (kg/mol)
PS125K			164.5		163.8	158.8	162.4
PS200K		238.1	237.3	235.0	236.0	231.4	235.6
PS226K		307.5	309.3		302.4	289.3	302.1
PS564K		683.0	689.5	661.5	667.1	649.0	670.0
PS1M	1167	1171	1190	1171	1146	1156	1167
PS2M	2723	2741	2909	2775	2757	2710	2769
PS4M	5024	4840	4905	4832[b]	4579[b]	4445[b]	4923
PS5M	5024	5316	5286	5040[b]	4807[b]	4664[b]	5209
PS7M	7345	7447	7469	7200[b]	6784[b]	6267[b]	7420
PS8M	8760	8611	8505	8328[b]	7950[b]	7434[b]	8625
PS10M	10110	9799	9987	9970[b]	9403[b]	8212[b]	9965
PS16M	14840	16650	16720	15890[b]	14550[b]	9764[b]	16070
PS14M	19880	19740	21800	19610[b]	15800[b]	9358[b]	20470

[a] Average values of M_w were taken over the values listed to the left. [b] These data were excluded before taking the average.

Table 3. $R_{g,z}$ of PS Standards Determined by HDC-MALLS at Different Flow Rates

	$R_{g,z}$ (nm) at flow rate (mL/min) of						
sample	0.025	0.05	0.10	0.30	0.50	1.00	av $R_{g,z}$[a] (nm)
PS125K			17.7		19.2	18.1	18.3
PS200K		20.3	19.6	19.7	20.2	20.1	20.0
PS226K		23.2	24.3		24.6	23.3	23.8
PS564K		33.7	34.6	34.2	35.2	34.8	34.5
PS1M	48.6	48.2	49.0	48.6	48.4	48.6	48.6
PS2M	82.2	82.9	83.1	82.0	82.5	82.3	82.5
PS4M	117.2	116.6	115.7	115.8[b]	116.1[b]	115.7[b]	116.5
PS5M	117.5	118.1	117.3	117.1[b]	116.7[b]	115.9[b]	117.6
PS7M	156.1	156.1	154.6	153.2[b]	149.7[b]	143.1[b]	155.6
PS8M	159.2	159.2	159.0	158.3[b]	157.2[b]	153.0[b]	159.1
PS10M	175.7	176.5	175.3	174.2[b]	172.6[b]	164.2[b]	175.8
PS16M	257.6	258.6	252.2	230.7[b]	239.1[b]	191.2[b]	256.1
PS14M	296.9	292.1	283.4	276.1[b]	273.4[b]	189.6[b]	290.8

[a] Average values of $R_{g,z}$ were taken over the values listed to the left. [b] These data were excluded before taking the average.

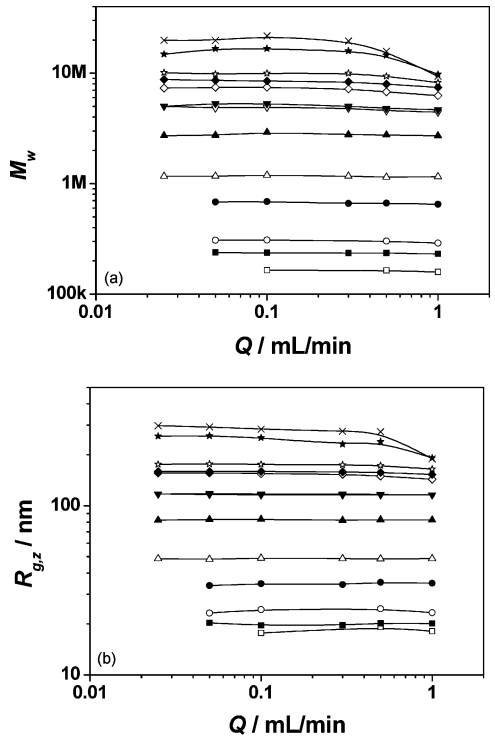

Figure 4. M_w (a) and $R_{g,z}$ (b) as a function of Q for all PS samples: □, PS125K; ■, PS200K; ○, PS226K; ●, PS564K; △, PS1M; ▲, PS2M; ▽, PS4M; ▼, PS5M; ◇, PS7M; ◆, PS8M; ☆, PS10M; ★, PS16M; ×, PS14M.

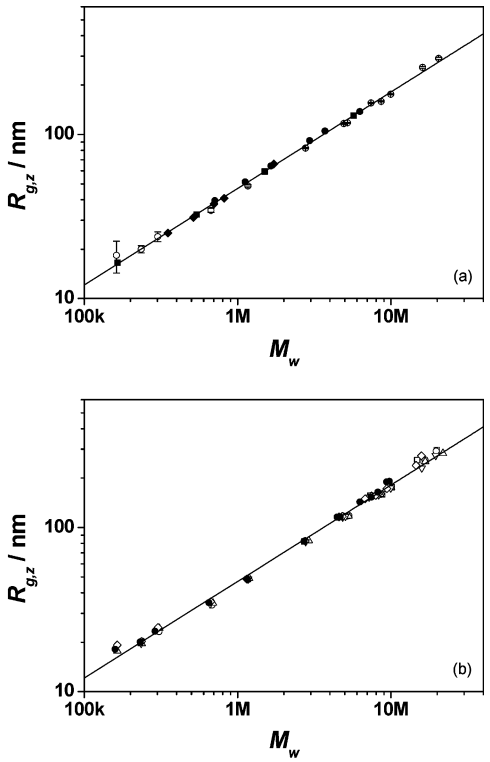

Figure 5. $R_{g,z}$ as a function of M_w for PS samples: (a) the data of the last columns of Tables 2 and 3 (○) and the data in references (■, Schulz and Baumann;[30] ●, Park and Chang;[31] ◆, Nakamura et al.[32]); (b) the data at different flow rates (□, 0.025; ○, 0.05; △, 0.10; ▽, 0.30; ◇, 0.50; ●, 1.00 mL/min). The straight lines indicate R_g (nm) = $0.0139M^{0.588}$.

to note that a shoulder with a much higher size of R_g = ~250 nm develops at flow rates less than 0.10 mL/min, while it is not observed at flow rates higher than 0.1 mL/min. Instead, a lower slope of R_g−V_e curve was observed, indicating that the large size fraction that can be separated at lower flow rates coeluted with the

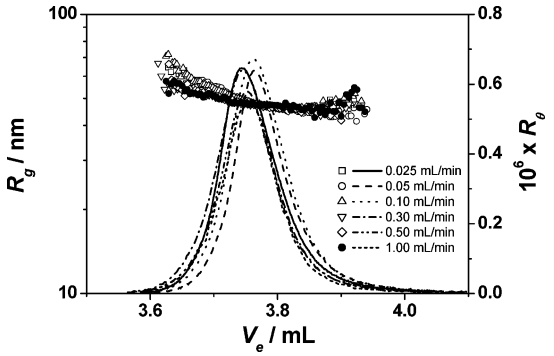

Figure 6. R_g as a function of V_e for PS1M obtained by columns packed with 15 μm particles at flow rates of 0.025, 0.05, 0.10, 0.30, 0.50, and 1.00 mL/min. The lines are the Rayleigh ratios of polymer at scattering angle of 90° at each V_e.

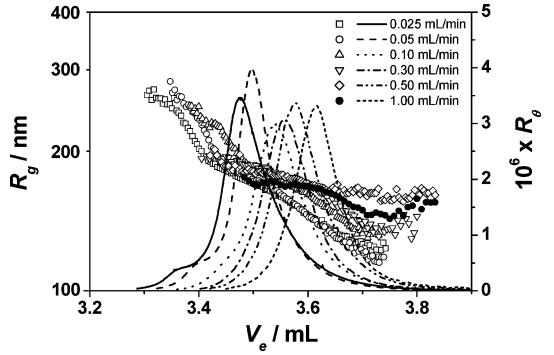

Figure 7. R_g as a function of V_e for PS10M obtained by columns packed with 15 μm particles at flow rates of 0.025, 0.05, 0.10, 0.30, 0.50, and 1.00 mL/min. The lines are the Rayleigh ratios of polymer at scattering angle of 16.8° at each V_e.

smaller size fraction at higher flow rates. This may be due to shear deformation and/or degradation of the large size fraction. From the obtained M_w and $R_{g,z}$ at different flow rates (Tables 2 and 3), there is only a slight degradation at flow rates of 0.50 and 1.00 mL/min for PS10M.

More interestingly, for PS14M with $M_w = 20.5$M, the chromatogram and the R_g–V_e curve showed more distinct dependences on flow rate, as shown in Figure 8. The chromatograms shift to higher elution volumes with increasing flow rate. In addition, a second peak with $R_g = \sim 340$ nm appeared at flow rate of 0.30 mL/min. This peak also shifts toward higher elution volume with increasing flow rate and broadens significantly. At flow rate of 1.00 mL/min, the second peak is only observed as a tailing with $R_g = \sim 235$ nm. The much lower M_w and $R_{g,z}$ of the overall sample indicates polymer degradation at this flow rate. The R_g–V_e curve at 0.025 mL/min clearly shows that this "narrow" standard was composed of PS chains with R_g ranging from 125 to 450 nm (with predominant components at $\sim 250 \pm 100$ nm). From the relationship between R_g and M, this corresponds to a molar mass range from 5.30M to 46.8M. It is not unexpected that such high molar mass PS standards are significantly broader than expected for a Poisson distribution due to the difficulties in anionic polymerization. At higher flow rates, unexpected R_g–V_e curves were obtained. At a flow rate of 0.05 mL/min, a constant value of R_g of ~370 nm was observed for the earliest eluting polymer fraction, and then R_g decreased with increasing V_e as anticipated for HDC separation. At flow rate of 0.10 mL/min, a

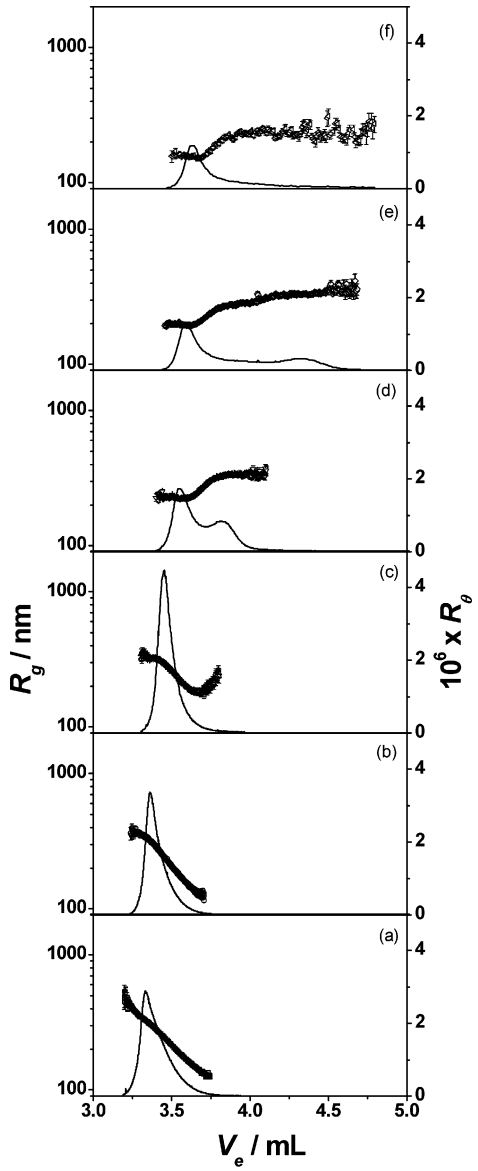

Figure 8. R_g as a function of V_e for PS14M obtained by columns packed with 15 μm particles at flow rates of 0.025 (a), 0.05 (b), 0.10 (c), 0.30 (d), 0.50 (e), and 1.00 mL/min (f). The lines are the Rayleigh ratios of polymer at scattering angle of 16.8° at each V_e.

similar R_g–V_e curve was observed with a plateau value of R_g of ~322 nm at low V_e region, then R_g decreased with increasing V_e until an increase at the end of the chromatogram. While at higher flow rate (>0.10 mL/min), a plateau value of R_g was also observed at low V_e region, but then R_g increased with increasing V_e to a second plateau value of R_g at the second peak of the chromatogram, which cannot be explained by HDC separation mechanism. In addition, the first plateau value of R_g decreased with increasing flow rate. Another high molar mass PS sample, PS16M with $M_w = 16.1$M showed a similar chromatographic behavior and R_g–V_e curves. It is interesting to note that the plateau values of R_g at the low V_e region for these two broad samples were nearly identical at the same flow rate, as listed in Table 4.

Such a flow rate dependence of the abnormal elution behavior of high molar mass PS might be explained as follows.

Table 4. First Plateau Value of R_g for PS14M and PS16M at Different Flow Rates

flow rate (mL/min)	R_g[a] (nm) of PS14M	R_g[a] (nm) of PS16M	R_g[b] (nm)
0.025			
0.05	369.6 (14.2)	380.9 (20.6)	375.2 (17.4)
0.10	322.5 (6.7)	318.0 (13.6)	320.2 (10.2)
0.30	229.8 (4.2)	229.7 (4.4)	229.7 (4.3)
0.50	198.3 (3.3)	196.5 (3.8)	197.4 (3.5)
1.00	158.8 (5.7)	159.6 (2.9)	159.2 (4.3)

[a] Average of the plateau values of R_g in the first plateau; mean standard deviation indicated in parentheses. [b] Average of PS14M and PS16M.

The elongational rate $\dot{\epsilon}$ in the packed column is

$$\dot{\epsilon} = k_1\left(\frac{\bar{v}}{d_p}\right) \tag{3}$$

where the superficial flow velocity $\bar{v} = Q/(\pi r^2)$ with Q and r being the flow rate and the column radius, respectively. d_p is the particle size, and k_1 is a parameter depending on packing structure with $k_1 = 21.68$ for randomly packed beds.[16]

The longest relaxation time τ for a polymer chain is given by[33]

$$\tau = \frac{C\eta R_g^{\,3}}{kT} \tag{4}$$

where C is a numerical factor of the order of 1, η is the solvent viscosity, R_g is the radius of gyration, k is Boltzmann's constant, and T is the temperature. From Chu's data on the relaxation of a single DNA molecule,[17−20] C was calculated to be 1.0 and was used in this study.

The Deborah number D_e can be calculated by

$$D_e = \tau\dot{\epsilon} = \frac{C\eta R_g^{\,3}}{kT} k_1\left(\frac{Q}{\pi r^2 d_p}\right) \tag{5}$$

A coil−stretch transition occurs when $\dot{\epsilon}$ is increased above the critical strain rate $\dot{\epsilon}_c$ of a polymer chain with size of R_g, i.e., when $D_e > B$.

For a polymer with a broad size distribution, at a certain flow rate, there exists a critical polymer size $R_{g,c}$ at which the elongational rate reaches its critical strain rate and a coil−stretch transition occurs. For polymer chains with $R_g < R_{g,c}$, the D_e is low and the polymer chains are kept in coiled state. The coiled polymer chains will flow through the packed columns in HDC mode; i.e., they will elute later than polymer chains with $R_g = R_{g,c}$, and the size of the eluted polymer chain decreases with increasing elution volume. For polymer chains with $R_g > R_{g,c}$, the D_e is high and the polymer chains are stretched. The stretched larger polymer chains will flow through the packed columns in SC mode; i.e, they will also elute later than polymer chains with $R_g = R_{g,c}$, and the size of the eluted polymer chain increases with increasing elution volume. Consequently, polymer chains having a size of exact $R_{g,c}$ will elute first of all, followed by the coeluting larger stretched polymer chains and the smaller coiled polymer chains. The larger stretched polymer chains will relax to the coiled state in the detector where the elongational rate is negligible. MALLS will determine a z-averaged radius of gyration for these two polymer chains of different sizes at each elution volume. The average size depends on the sizes and compositions of the coeluting species. For a chain with R_g slightly larger than $R_{g,c}$ and a chain with R_g slightly smaller than $R_{g,c}$, both eluted slightly later than the chain with $R_g = R_{g,c}$, their average would be a value close to $R_{g,c}$. This explains the first plateau in the R_g−V_e curve for the earliest eluting polymer fraction at higher flow rates. For a polymer chain with R_g much larger than $R_{g,c}$, the elongational rate in the columns is much greater than its critical strain rate. The chain will be highly stretched and eluted much later, together with the coiled polymer chains of much lower R_g. This explains the increase of R_g at the end of the chromatogram and the appearance of a second peak with a large R_g.

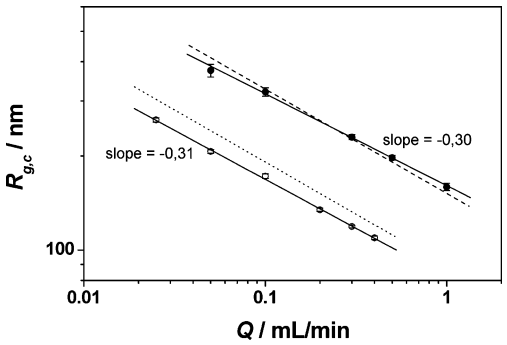

Figure 9. $R_{g,c}$ as a function of Q for PS flowing through columns packed with 15 μm (●) and 3 μm (○) particles. The dashed line and the dotted line were calculated according to eq 5 with $D_e = 0.50$ for columns packed with 15 μm particles and 3 μm particles, respectively.

At the lowest flow rate (0.025 mL/min), the elongational rate in the columns is 36.2 s^{-1} as calculated from eq 3, while the lowest critical strain rate for the largest chain with R_g = 450 nm of PS14M is 55.6 s^{-1} as calculated from eqs 1 and 4. At this flow rate, the elongational rate is weak for all species of PS14M, and there is no coil−stretch transition. All polymer chains of different size are in coiled state and flow through the columns in HDC mode. As the flow rate raises to 0.05 mL/min, the elongational rate (72.5 s^{-1}) is above the critical strain rate for the larger polymer chains, and they are stretched, while the elongational rate is still below the critical strain rate for the smaller polymer chains, and they are in coiled state. As the flow rate raises further, more and more polymer chains of lower size are stretched and flow through the columns in SC mode.

On the other hand, the plateau value of R_g for the earliest eluting polymer fraction gives an estimate of the critical size $R_{g,c}$ for a coiled polymer chain just begin to become stretched at a certain elongational rate. By plotting log $R_{g,c}$ vs log Q (Figure 9), a linear relationship was obtained, which was very close to the line calculated according to eq 5 with $D_e = 0.5$. The slope of −0.30 is slightly less than the theoretical value of −1/3.

Table 5 presents the elongational rate $\dot{\epsilon}$ in the columns at different flow rates, the relaxation time τ of the PS chain with size of $R_{g,c}$, and its Deborah number D_e, which were calculated according to eqs 3−5, respectively. The calculated critical Deborah number D_e, for PS chains with size of $R_{g,c}$ just begin to stretch at the elongational rate $\dot{\epsilon}$ in the HDC columns, ranged from 0.38 to 0.58 with an average value of 0.50, which agreed with theory and other experiments. This strongly supports that the HDC → SC transition in a packed column is induced by coil−stretch transitions of the polymer

Table 5. Q, $\dot{\epsilon}$, $R_{g,c}$, τ, and D_e at Different Flow Rates

Q (mL/min)	$\dot{\epsilon}$ (1/s)	$R_{g,c}$ (nm)	τ (ms)[a]	D_e[a]
0.025	36.2			
0.05	72.5	375.2	5.21 (0.73)	0.378 (0.053)
0.10	145	320.2	3.24 (0.31)	0.470 (0.045)
0.30	435	229.7	1.20 (0.07)	0.520 (0.029)
0.50	725	197.4	0.76 (0.04)	0.550 (0.029)
1.00	1450	159.2	0.40 (0.03)	0.577 (0.047)

[a] Mean standard deviation indicated in parentheses was calculated from the deviation of $R_{g,c}$.

chains. In addition, the transition of chromatography mode from HDC to SC may provide a new method to study the coil−stretch transition of polymers in elongational flow through packed beds.

In molar mass or molecular size determination of high molar mass polymers by packed-column HDC or SEC, such a chromatography mode transition must be avoided since polymers cannot be separated effectively if HDC (or SEC) and SC both exist. The transition depends on both molecular size and flow rate. Therefore, for a high molar mass polymer sample, packed-column HDC must be performed at such a sufficiently low flow rate that the elongational rate in the column is less than the critical strain rate for all species in the sample. As shown in Figure 8, at a flow rate of 0.025 mL/min, SC was not observed for PS14M (it does exist, but only for polymer with R_g > 475 nm as extrapolating from the straight line in Figure 9, but this sample does not contain species of such a large size), but the separation needs 4 h. At a flow rate of 0.05 mL/min, the analysis is reduced to 2 h, but only species of R_g < 375 nm can be analyzed by HDC. Polymer chains with R_g > 375 nm, which only constitute a small amount of PS14M, were stretched and eluted in SC mode, they are only slightly stretched and coeluted for the earliest eluting polymer fraction. At a flow rate of 0.10 mL/min, polymer chains with R_g > 320 nm were stretched, the increasing R_g at the end of chromatogram is due to the elution of a small amount of highly stretched larger polymer molecules. For stretched polymer chains, at the same flow rate, the larger the polymer size, the more the polymer is stretched and the later it is eluted from the column. While for polymer chains with the same size, the higher the flow rate, the more it is stretched and the later it is eluted from the column. At higher flow rates, the greatly stretched larger polymer chains eluted in SC mode can be separated from the coiled or slightly stretched smaller chains as shown by the second peak with R_g = ~340 nm at flow rates of 0.30 and 0.50 mL/min. As the flow rate is increased further, the elongational rate in the column reached the critical strain rate for the large polymer chain to fracture.[15] Some large polymer chains may be degraded, as proved by a tailing with R_g = ~235 nm in the R_g−V_e plot at flow rate of 1.00 mL/min, which agreed with its much lower M_w and $R_{g,z}$ (Tables 2 and 3). It should be noted that the size of the degraded chain (235 nm) is about 0.7 times of that of the original chain (340 nm), i.e., about 0.5 times in molar mass, which agrees with chain scission by half in elongational flow as had been observed in other experiments.[15]

The shoulder with R_g = ~250 nm for PS10M which was separated at low flow rate (Figure 7), was not observed at a flow rate higher than 0.10 mL/min, since they are stretched and eluted in SC mode at high flow rates. The plateau value of R_g for the earliest eluting polymer fraction at high flow rates is slightly different from those determined by PS14M and PS16M. It could

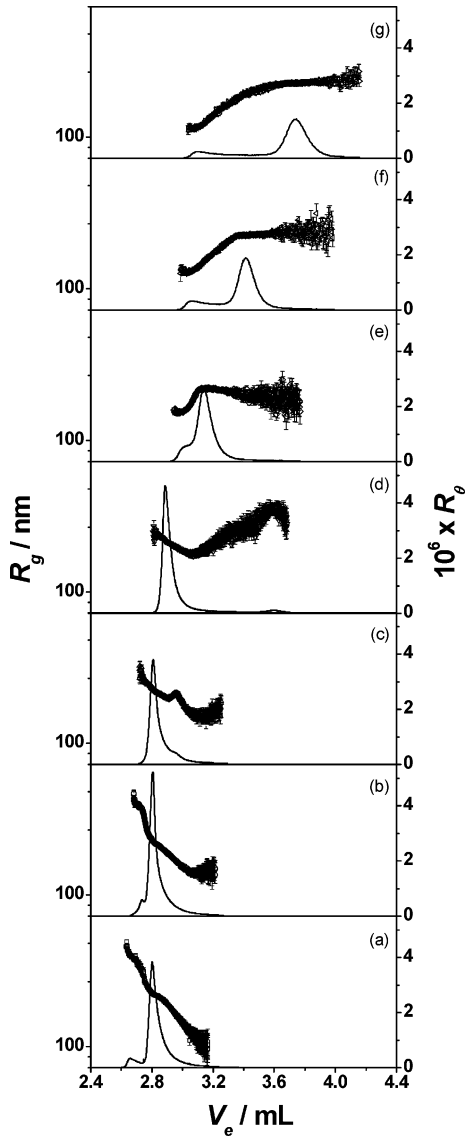

Figure 10. R_g as a function of V_e for PS10M obtained by columns packed with 3 μm particles at flow rates of 0.010 (a), 0.025 (b), 0.05 (c), 0.10 (d), 0.20 (e), 0.30 (f), and 0.40 mL/min (g), respectively. The lines are the Rayleigh ratios of polymer at scattering angle of 16.8° at each V_e.

be due to the discontinuous distribution of polymer size for PS10M in this size range, as seen by the drastic decrease from 250 to 190 nm in the R_g−V_e curve in Figure 7. In other experiments with more efficient HDC columns packed with 3 μm cross-linked polystyrene−divinylbenzene nonporous particles (with the same column dimensions as the columns packed with 15 μm particles), the shoulder with R_g = ~250 nm was fully separated as a peak from the smaller size fraction at an extremely low flow rate of 0.010 mL/min, as shown in Figure 10a.

Figure 10 shows the chromatograms and the R_g−V_e curves of PS10M at flow rates of 0.010, 0.025, 0.05, 0.10, 0.20, 0.30, and 0.40 mL/min obtained with the columns packed with 3 μm particles. Similar to the elution behaviors of PS14M obtained with the columns packed with 15 μm particles (Figure 8), the chromatograms of PS10M obtained with the columns packed with 3 μm particles shift to higher elution volumes with increasing flow rate. A second peak with R_g = ~178 nm develops at flow rates of 0.2 mL/min, and this peak also shifts toward higher elution volumes with increasing flow rate.

M_w and $R_{g,z}$ of the whole sample obtained at different flow rates indicated no obvious degradation at high flow rates. A plateau value of R_g for the earliest eluting polymer fraction appears at high flow rates. The critical size $R_{g,c}$ for the HDC → SC transition in the columns packed with 3 μm particles is determined in the same way as above and is also plotted as a function of Q in Figure 9. A linear relationship between log $R_{g,c}$ and log Q with a slope of −0.31 is obtained. It can be seen that the HDC → SC transition occurs for smaller polymer molecules in the columns packed with 3 μm particles at the same flow rate. This is easily understood since the elongational rate in the columns is inversely proportional to the size of the packing particles, according to eq 3. At the same flow rate, the elongation rate in the columns packed with smaller particles is larger, and polymer molecules with smaller sizes will be stretched. It should be noted that the log $R_{g,c}$−log Q curve obtained for columns packed with 3 μm particles is below the line calculated according to eq 5 with $D_e = 0.50$. The average critical Deborah number D_e, calculated from $R_{g,c}$ and Q data for the columns packed with 3 μm particles, is 0.35, which is slightly less than that obtained for columns packed with 15 μm particles (0.50). This is because the critical Deborah number D_e obtained from HDC → SC transition is a reflection that the polymer chains are stretched to such an extent that they exhibit problems (to be retarded) during passing through the tortuous narrow channels between the particles. It is reasonable that for polymer coils with a given size, it requires a less extension in the columns packed with smaller particles to have such problems. Thus, the critical Deborah number D_e is less for columns packed with smaller particles, since the steady-state extension of a given polymer chain increases with increasing D_e.

It can be seen from Figure 10 that at high flow rates the greatly stretched larger PS chains with $R_g = \sim 178$ nm eluted in SC mode can be separated from the smaller PS chains eluted in HDC mode. It suggests that the HDC → SC transition can be used to remove the smaller fraction from the high molar mass polymers. This provides a method to prepare high molar mass polymer standards with extremely narrow molar mass distribution. Theoretically speaking, the HDC → SC transition can be applied to separate linear polymer chains and branched polymer chains or branched polymer chains with different topologies of the same molar mass. By selecting the packing particle size, flow rate, temperature, and solvent viscosity according to the sizes of linear and branched chains, the elongational rate in the column can be adjusted to be larger than the critical strain rate for the linear chains, while it is still below the critical strain rate for the branched chain. The linear chains will stretch and elute in SC mode, while the branched chains will stay in coiled state and elute in HDC (or SEC) mode.

This SEC → SC transition and HDC → SC transition for DNA had been found to be dependent on the packing particle size, flow rate, molecular size, temperature, and solvent viscosity.[23−25] In fact, the results are in accordance with the theory of coil−stretch transition of polymers at critical D_e, since the former two parameters were related to $\dot{\epsilon}$, while the latter three parameters were related to τ; any factors that increased D_e would make SC effect more prominent.

The obtained log $R_{g,c}$−log Q curves together with eq 5 can serve as a guidance to avoid chromatography mode transition in packed-column HDC of high molar mass polymers. The maximum flow rate for a given polymer size at a given particle size can be calculated according to eq 5. In HDC packed with smaller particles, a much lower flow rate must be employed to avoid coil−stretch transition of high molar mass polymers. As predicted from eq 5, increasing the size of the analyte by a factor of 2 will demand decreasing the flow rate by a factor of 8, decreasing the particle size by a factor of 2 will require decreasing the flow rate by a factor of 2, to avoid the HDC → SC transition. It also indicated that increasing temperature and/or decreasing eluent viscosity alleviate the SC effect. These effects are in further study. It would also be interesting to study the SEC → SC transition of high molar mass polymers, which is also under investigation.

Conclusions

A series of PS standards were studied by packed-column HDC coupled with a multiangle laser light scattering (MALLS) detector at different eluent flow rates. The abnormal elution behaviors and the unexpected R_g−V_e curves for high molar mass PS were interpreted in terms of HDC → SC transition induced by coil−stretch transition. The flow rate dependence of the HDC → SC transition was explained by coil−stretch transitions of polymer molecules in elongational flow. The transition of chromatography mode may provide a new method to study the coil−stretch transition of polymers in elongational flow through packed beds. For high molar mass polymer samples, HDC must be performed at flow rates sufficiently low that the elongational rate in the column is less than the critical strain rate for coil−stretch transition to occur for all species in the sample. The HDC → SC transition can be used to prepare high molar mass polymer standards with extremely narrow molar mass distribution. It also shows potential possibility in separating linear polymer chains and branched polymer chains or branched polymer chains with different topologies of the same molar mass.

Acknowledgment. The authors thank Mr. Adrian Williams (Polymer Laboratories Ltd.) for kindly supplying the columns.

Supporting Information Available: Fit method of MALLS data for high molar mass polymers, instrumental band broadening on the determination of M, R_g, and the average M_w and $R_{g,z}$ of the whole sample, molar mass distribution of PS14M, and the longest relaxation time of polymer. This material is available free of charge via the Internet at http://pubs.acs.org.

References and Notes

(1) Yau, W. W.; Kirkland, J. J.; Bly, D. D. *Modern Size Exclusion Liquid Chromatography;* Wiley: New York, 1979.
(2) Giddings, J. C. *Unified Separation Science;* Wiley-Interscience: New York, 1991.
(3) Small, H. *Acc. Chem. Res.* **1992**, *25*, 241.
(4) Small, H. *J. Colloid Interface Sci.* **1974**, *48*, 147.
(5) Langhorst, M. A.; Stanley, Jr., F. W.; Cutié, S. S.; Suggarman, J. H.; Wilson, L. R.; Hoagland, D. A.; Prud'homme, R. K. *Anal. Chem.* **1986**, *58*, 2242.
(6) Hoagland, D. A.; Prud'homme, R. K. *J. Appl. Polym. Sci.* **1988**, *36*, 935.
(7) Stegeman, G.; Oostervink, R.; Kraak, J. C.; Poppe, H. *J. Chromatogr.* **1990**, *506*, 547.
(8) Stegeman, G.; Kraak, J. C.; Poppe, H.; Tijssen, R. *J. Chromatogr. A* **1993**, *657*, 283.

(9) Stegeman, G.; Kraak, J. C.; Poppe, H. *J. Chromatogr.* **1991**, *550*, 721.
(10) Venema, E.; Kraak, J. C.; Poppe, H.; Tijssen, R. *J. Chromatogr. A* **1996**, *740*, 159.
(11) Tijssen, R.; Bos, J.; van Kreveld, M. E. *Anal. Chem.* **1986**, *58*, 3036.
(12) De Gennes, P. G. *J. Chem. Phys.* **1974**, *60*, 5030.
(13) Larson, R. G.; Magda, J. J. *Macromolecules* **1989**, *22*, 3004.
(14) Malika, J. M.; Hoagland, D. A. *Macromolecules* **1991**, *24*, 3427.
(15) Keller, A.; Odell, J. A. *Colloid Polym. Sci.* **1985**, *263*, 181.
(16) Hass, R.; Durst, F. *Rheol. Acta* **1982**, *21*, 566.
(17) Perkins, T. T.; Smith, D. E.; Chu, S. *Science* **1997**, *276*, 2016.
(18) Smith, D. E.; Chu, S. *Science* **1998**, *281*, 1335.
(19) Smith, D. E.; Babcock, H. P.; Chu, S. *Science* **1999**, *283*, 1724.
(20) Schroeder, C. M.; Babcock, H. P.; Shaqfeh, E. S. G.; Chu, S. *Science* **2003**, *301*, 1515.
(21) Hirabayashi, J.; Kassi, K. *Anal. Biochem.* **1989**, *178*, 336.
(22) Huber, C. G. In *Encyclopedia of Analytical Chemistry*; Meyers, R. A., Ed.; John Wiley & Sons: Chichester, 2000; pp 11250−11278.
(23) Hirabayashi, J.; Ito, N.; Noguchi, K.; Kassi, K. *Biochemistry* **1990**, *29*, 9515.
(24) Hirabayashi, J.; Kassi, K. *J. Chromatogr. A* **2000**, *893*, 115.
(25) Peyrin, E.; Caron, C.; Garrel, C.; Ravel, A.; Villet, A.; Alary, J.; Grosset, C.; Favier, A. *Talanta* **2001**, *55*, 291.
(26) Hoagland, D. A.; Prud'homme, R. K. *Macromolecules* **1989**, *22*, 775.
(27) Andersson, M.; Wittgren, B.; Wahlund, K. G. *Anal. Chem.* **2003**, *75*, 4279.
(28) Noda, I.; Imai, M.; Kitano, T.; Nagasawa, M. *Macromolecules* **1983**, *16*, 425.
(29) Freire, J. J.; Álvarez, G.; Bishop, M. *Macromol. Theory Simul.* **2002**, *11*, 11.
(30) Schulz, G. V.; Baumann, H. *Makromol. Chem.* **1968**, *114*, 122.
(31) Park, S.; Chang, T. *Macromolecules* **1991**, *24*, 5729.
(32) Nakamura, Y.; Wan, Y.; Mays, J. W.; Iatrou, H.; Hadjichristidis, N. *Macromolecules* **2000**, *33*, 8323.
(33) Doi, M.; Edwards, S. F. *The Theory of Polymer Dynamics;* Oxford University Press: Clarendon, 1986.

MA050964G